Cellulose (2019) 26:8367–8381
https://doi.org/10.1007/s10570-019-02712-6

ORIGINAL RESEARCH

Characteristic microcrystalline cellulose extracted by combined acid and enzyme hydrolysis of sweet sorghum

Haiwei Ren · Jiali Shen · Jiawen Pei · Zhiye Wang · Zhangpu Peng · Shanfei Fu · Yi Zheng

Received: 28 January 2019 / Accepted: 22 August 2019 / Published online: 12 September 2019

Abstract Microcrystalline cellulose (MCC) has been widely used in medicine, food and cosmetic industries. In this study, a combination method by using hydrochloric acid hydrolysis and fibrolytic enzyme purification was studied to extract MCC from sweet sorghum. The response surface methodology was employed to optimize the hydrochloric acid hydrolysis condition and therefore to maximize the MCC yield and cellulose content (purity). The optimal conditions for the hydrochloric acid hydrolysis were determined to be acid concentration of 7.0%, liquid–solid ratio of 17.3:1, time of 90 min, and temperature of 40 °C. Under such conditions, the yield and cellulose content of acid-extracted MCC were 81.8% and 93.2%, respectively. For enzyme refining of acid-extracted MCC, the optimum conditions were enzyme dosage of 4000 U/g substrate and time of 2 h, with which the yield, cellulose content and DP of the refined MCC were 80.03%, 99.80% and 287, respectively which were comparable to that of the commercial MCC (Lowa®PH101). Scanning electron microscopy, X-ray diffraction, Fourier transmission infrared spectroscopy, thermogravimetric analysis (TGA), and ^{13}C NMR were used to characterize the

Electronic supplementary material The online version of this article (https://doi.org/10.1007/s10570-019-02712-6) contains supplementary material, which is available to authorized users.

H. Ren · J. Shen · J. Pei
School of Life Science and Engineering, Lanzhou University of Technology, Langongping Road, Lanzhou 730050, Gansu Province, People's Republic of China
e-mail: rhw52571119@163.com

H. Ren · Z. Wang · Z. Peng
Institute of Biology, Gansu Academy of Sciences, South Dingxi Road, Lanzhou 730000, Gansu Province, People's Republic of China

S. Fu (✉)
School of Environment and Civil Engineering, Jiangnan University, No 1800, Lihu Avenue, Wuxi 214122, Jiangsu Province, People's Republic of China
e-mail: fusf@jiangnan.edu.cn

Y. Zheng
Department of Grain Science and Industry, Kansas State University, 101C BIVAP, 1980 Kimball Avenue, Manhattan, KS 66506, USA

refined MCC. The refined MCC demonstrated rod-shaped morphologies, and had a series of characteristic absorption peaks and chemical groups pertain to cellulose as similar to the Lowa®PH101. The X-ray diffraction pattern and ^{13}C NMR spectrum reflected that the refined MCC had typical cellulose I structure. TGA indicated that the refined MCC had good thermal stability. This study showed sweet sorghum is a potential low-cost raw material for MCC production, and the combined acid-enzyme extraction method is promising to extract high purity MCC from cellulosic substrate.

Keywords Sweet sorghum · Microcrystalline cellulose · Response surface methodology · Structural characterization

Introduction

The development of new types of "green" bio-based and biodegradable materials from natural sources has received increasing interest from research community and the public. Cellulose obtained from lignocellulosic biomass, a long chain carbohydrate polymer with repeated glucose units, is the most abundant biological macromolecule in nature (Hamid et al. 2014). The favorable properties of high mechanical strength, good thermal resistance and low cost for cellulose make it a promising alternative to petroleum, which can produce novel bio-based materials in a sustainable and environmentally-friendly way (Kian et al. 2017; Collazo-Bigliardi et al. 2018). Natural cellulose can be transformed into micro- and nano-scale materials, such as microcrystalline cellulose (MCC), which is a white, odorless, porous, non-fibrous, and crystalline powder. The depolymerization process can mainly remove amorphous regions of cellulose fibers, while leaving most crystalline structure intact (Hamid et al. 2014; Ilyas et al. 2018). To date, MCC has been widely used in food, cosmetics and pharmaceutical industries owing to its excellent properties including high thickeners, dispersing agents, flow controllers, and anti-caking agents (Sheng et al. 2018).

In general, the industrial MCC is mainly obtained from wood (e.g., hardwood and cork) and non-wood materials (e.g. waste cotton fabrics/velvet) (Nsor-Atindana et al. 2017). In addition, it has been reported that MCC can be produced from diverse low-cost and readily available by-products from agriculture or food processing, such as soybean hull (Merci et al. 2015), rice straw (Ilindra and Dhake 2008), corn cobs (Azubuike and Okhamafe 2012), fodder grass (Kalita et al. 2013), cotton gin waste (Das et al. 2009), coffee husk (Collazo-Bigliardi et al. 2018), distillers grains (Ren et al. 2015), and others agricultural residues (Elsakhawy and Hassan 2007). Based on the origin of cellulose source and extraction method/conditions, the obtained MCC would possess different physicochemical properties and performance in terms of compatibility, degree of crystallinity, mechanical properties, specific surface area, and thermal stability, etc. (Chuayjuljit et al. 2010; Kambli et al. 2017). Sweet sorghum [*Sorghum bicolor* (L.) *Moench*] is an annual C4 crop with fast growth rate and high biomass yield. Sweet sorghum can adapt to almost all temperate and tropical climates as an annual or short perennial crop, tolerate to saline and drought conditions, and grow in marginal land (Li et al. 2014; Wu et al. 2015; Jiang et al. 2019). Therefore, sweet sorghum might provide a versatile crop to produce human food (Anglani 1998), bioenergy (Regassa and Wortmann 2014), livestock feed (Fazaeli et al. 2006), and fiber (Murray et al. 2009). The juice squeezed from fresh sweet sorghum contains a large amount of fermentable sugar (sucrose, glucose and fructose) and many essential trace elements suitable for microbial growth and ethanol production (Ariyajaroenwong et al. 2012). However, sweet sorghum unharvested timely were withering and air-dried in field, resulting in severe lignifying and unavailability of free sugars by squeeze to bioenergy or bio-refinery. How to effectively utilize the air-dried sweet sorghum is a heave problem at present. The high content of cellulose in sweet sorghum offered the opportunity for utilization. However, little information is available about MCC isolation from sweet sorghum, which limits a potential as a new sustainable feedstock to produce biodegradable bio-based materials for sweet sorghum.

MCC can be extracted from native cellulose by partial depolymerization via chemical (e.g., mineral acid hydrolysis, hydrothermal, ionic liquid, metal ions enhanced high temperature liquid water, etc.), biological (e.g., enzymatic hydrolysis), mechanical techniques (high-pressure homogenization, irradiation), and combination of two or more of these techniques (Agblevor et al. 2007; Vanhatalo et al. 2016; Nsor-

Atindana et al. 2017). Of all above-mentioned methods, mineral acid hydrolysis is a conventional choice. However, high amount of acids or higher temperature leads to severe equipment corrosion and environmental issues (Trache et al. 2014). In addition, the acid-extracted MCC often holds a low purity, which needs further purification. Enzyme, such as cellulase, has also been used to prepare and control the morphology of the MCC. However, high cost and poor efficiency limit the utilization of enzyme in MCC preparation (Agblevor et al. 2007; Ibrahim et al. 2013). Therefore, it is essential to develop a more environmental friendly method for the high purity MCC extraction as little chemical reagent as possible.

In this study, a novel method by combing hydrochloric acid (HCl) and fibrolytic enzyme hydrolysis (i.e., acid and enzyme hydrolysis were conducted sequentially) was used to extract MCC from sweet sorghum, which could achieve high purity MCC while reducing the acid concentration and the dose of enzyme for MCC extraction with very minimum catalyst usage. In the acid extraction step, the extraction conditions including temperature, time, liquid/solid (L/S) ratio, and acid concentration were optimized by using response surface methodology (RSM) in response to the yield, cellulose content and polymerization degree (DP). Furthermore, the acid-extracted MCC was further purified by fibrolytic enzyme to obtain refined MCC which were subject to a series of analyses, including scanning electron microscopy (SEM), X-ray diffraction, Fourier transmission infrared (FTIR) spectroscopy, thermogravimetric analysis (TGA), and ^{13}C nuclear magnetic resonance spectroscopy (NMR). The properties of refined MCC were compared with the commercial MCC (Lowa®PH101).

Materials and methods

Materials

The air-dried sweet sorghum stalk was obtained from a farmland near Lanzhou (Lanzhou, Gansu, China), which was milled directly in a hammer mill to pass through a 1-mm screen in order to obtain a homogeneous particle size. The milled sweet sorghum stalk particles were dried to a constant weight at 105 °C and stored in plastic bags until further processed. The main chemical components (dry basis) of sweet sorghum stalk included cellulose (33.75%), hemicellulose (19.71%), lignin (23.44%), soluble sugars (17.70%) and protein (5.26%). The commercial MCC, Lowa®-PH101 was purchased from E Hua Pharmaceutical Co., Ltd. (Liaocheng, Shandong, China) and used as a comparison reference. The fibrolytic enzyme (including cellulase and xylanase, the total enzymatic activity was 5.0×10^4 U/g) was purchased from Imperial Jade Bio-technology Co., Ltd (Yinchuan, Ningxia, China). All other chemicals were all laboratory grade unless stated, otherwise.

Preparation of crude cellulose from sweet sorghum stalk

The air-dried sweet sorghum stalk samples were boiled in deionized water at 100 °C for 3 h with the solid/liquid ratio of 1:30 (g/mL). After cooling to 25 °C, the cooking liquor was centrifuged at 3,000 rpm for 10 min and the supernatant was discarded. The cooked stalk solid was collected and mixed with 0.03 g/mL NaOH for 70 min at 50 °C for alkali pretreatment, in which the ratio of NaOH solution to the cooked stalk (wet weight) was 14:1 (mL/g). Subsequently, the suspension was centrifuged at 3000 rpm for 10 min and the pellets were washed with deionized water until the pH of filtrate was neutral. The alkali-pretreated stalk samples were bleached with 10 mL Na_2SO_3 (0.03 g/mL) and 15 mL NaClO (0.06 g/mL) in sequence at 80 °C for 120 min. Afterwards, the bleached stalk samples were washed with deionized water by centrifugation until the pH of eluate was neutral. The above-mentioned bleaching and washing processes were repeated for 5 times until the samples were nearly white to obtain crude cellulose.

Preparation of MCC by using combined acid and enzymatic hydrolysis

Factor screening for acid extraction of MCC from crude cellulose

The crude cellulose obtained from "Preparation of crude cellulose from sweet sorghum stalk" section was first subject to HCl extraction of MCC. During this acid extraction, four operation parameters were studied to determine their significance, including acid

concentration [1, 3, 5, 7, and 9% (wt%)], temperature (20, 40, 60, 80, and 100 °C), L/S ratio (30:1, 25:1, 20:1, 15:1, and 10:1, mL/g, dry basis), and time (30, 50, 70, 90, and 110 min). The crude cellulose was mixed with acid solution in a sealed reactor, heated to desired temperature and held for designated time. The agitation speed was kept at constant of 30 rpm during hydrolysis. Upon the finish of hydrolysis, the hydrolyzed cellulose sample was washed several times with distilled water by centrifugation at 3900 rpm for 30 min to remove acid. After washing, the recovered solid cellulose residues were dried in a vacuum oven at 60 °C for 6 h and weighed to measure the yield of MCC. The obtained MCC samples were stored for physicochemical analysis afterwards. In each experiment, one factor was variable and the other factors were kept constant on the basis of preliminary experiment. The yield and the purity (i.e., cellulose content) of the acid-extracted MCC were used to evaluate the extraction efficiency. The yield of MCC was calculated as Eq. (1).

$$MCC\ yield(\%) = \frac{Mass\ of\ acid\ extraction\ MCC\ product\ (g)}{Mass\ of\ cellulose\ in\ raw\ stalk\ (g)} \times 100\% \quad (1)$$

Cellulose content was determined by using the Updegraff's method with slight modification (Updegraff 1969). The standard curve was made with pure cellulose (Lowa®PH101). In measurement, 0.5 mL of 2% anthrone reagent was added to the sample (0.3 g, dry weight) in test tubes and 5 mL concentrated sulfuric acid was added slowly along the tube wall. The test tubes were sealed with plugs, and vortexed thoroughly followed by standing for 12 min. The absorbance was then measured at $\lambda = 620$ nm at a spectrophotometer (UV1901 and Shanghai Scientific Instrument Co., Ltd), and the cellulose content was calculated.

The degree of polymerization (DP) of the acid-extracted MCC was determined via viscosity measurement of the MCC samples dissolved in a cuprietheylenediamine (CED) solution using Cannon-Fenske viscometer (Wang et al. 2010). Every measurement was performed in triplicate. The DP was calculated based on Eq. (2).

$$DP = 95 \times [\eta]\frac{c}{w} \quad (2)$$

where w is the dry weight (g) of the MCC sample; c is the MCC concentration (g/mL) in 0.5 M CED solution, and $[\eta]$ is the intrinsic viscosity (mL/g) of the solution dissolved MCC.

Optimization of MCC extraction by acid hydrolysis

Based on the factor screening results from "Factor screening for acid extraction of MCC from crude cellulose" section, the acid concentration, temperature and L/S ratio were determined to be significant factors influencing the yield and purity (cellulose content) of MCC during acid hydrolysis. Therefore, the Box–Behnken design (BBD) of RSM with three-factor and three-level (i.e., 3^3) was used to optimize the acid hydrolysis parameters in response to MCC yield and cellulose content. The parameters and their levels were presented in Table 1. The statistical analysis of experimental data was conducted by using Design Expert (Version 8.06, Stat-Ease Inc., Silicon Valley, CA, USA), and the data were fitted using the liner regress model (Eq. 3) (Gu et al. 2017):

$$Y = \beta_0 + \sum_{i=1}^{3}\beta_i X_i + \sum_{i=1}^{3}\beta_{ii}X_i^2 + \sum_{i=1}^{3}\sum_{j=i+1}^{3}\beta_{ij}X_iX_j \quad (3)$$

where Y is the predicted response (yield and cellulose content), β_0 is the model constant, and β_i, β_{ii}, and β_{ij} represent the coefficient of linear, quadratic and interaction coefficients, respectively. X_1, X_2 and X_3 correspond to the independent variables (Table 1). This model evaluates the effects of each variable and their interactions on the responses. The analysis of variance (ANOVA) was used to test the adequacy of the developed model and statistical significance of the regression coefficients. The response surface contour plots were used to analyze the interactions among the variables and their corresponding effects (Wang et al. 2015). Thrice additional experiments were subsequently conducted to verify the optimum conditions.

Purification of acid-extracted MCC by using fibrolytic enzyme treatment

The fibrolytic enzyme was used to remove impurities and improve the purity of acid-extracted MCC. The effects of enzyme dose and enzymolysis time on the

Table 1 Box–Behnken design (BBD) for acid hydrolysis

Factors	Code	Level		
		− 1	0	1
(A) L/S ratio (mL/g)	X_1	15:1	20:1	25:1
(B) Temperature (°C)	X_2	40	60	80
(C) Hydrochloric acid concentration (wt%)	X_3	5	7	9

yield and purity were examined. The solid MCC substrates (10.0 g, dry weight) from the optimum acid extraction MCC of in "Optimization of MCC extraction by acid hydrolysis" section were enzymatic hydrolyzed with 0.02 g, 0.04 g, 0.06 g, 0.08 g, and 0.1 g of fibrolytic enzyme in sodium acetate buffer at pH 5.0. The reaction was carried out in a shaking water bath at 50 °C and 65 rpm for 2 h, 4 h, 6 h, and 8 h. The enzymatic hydrolysis was stopped by boiling the samples for 10 min to deactivate the enzymes. The mixture was vacuum-filtered and washed thoroughly with deionized water to obtain solid samples, which was finally oven-dried at 60 °C and ground into fine powder using mortar and pestle to obtain the refined MCC.

Characterization of MCC

SEM analysis

SEM imaging was done by using JSM-5600LV scanning electron microscope (Jeol Instruments, Tokyo, Japan). Samples were prepared by dispersing dry powder on double-sided conductive adhesive tape and coated with carbon with arc discharge method. All samples were sputtered with gold before the microscopic observations were obtained (Kiziltas et al. 2014). Samples were scanned in secondary electrons for morphology with an accelerating voltage of 20 kV.

FTIR analysis

The dried samples were embedded in KBr pellets and analyzed by using a Nexus 670 (Thermo Nicolet Corporation) FTIR spectrometer. The spectra were recorded in transmittance band mode in the range of 4000–500 cm^{-1} with 32 scans in order to achieve an acceptable signal-to-noise ratio. In all analyses, spectra resolution was maintained at 4 cm^{-1}.

X-ray diffraction (XRD) analysis

The diffraction patterns were obtained using a high resolution Rigaku X-ray diffractometer (D/max-2400, Rigaku) with a scanning speed of 1°/min. The diffraction patterns were recorded using Cu-Kα radiation (wavelength 1.541 Å) operating with Ni filter from 0° to 80° of 2θ (scanning angle) at accelerating voltage of 40 kV and current of 100 mA.

The patterns were further normalized and the analyzed using the pseudo-Voigt peak shape with the Maud Rietveld program (Materials Analysis Using Diffraction, version 2.7). The crystallinity was calculated from the area of the calculated pattern for crystalline cellulose divided by the sum of the areas for crystalline and amorphous regions. The d-spacings were calculated from refined unit cell dimensions and crystallite sizes perpendicular to different lattice planes were calculated using the Scherrer Eq. (4).

$$L_{hkl} = \frac{0.9\lambda}{B_{hkl}\cos\theta} \tag{4}$$

where λ is the X-ray wavelength; B_{hkl} is the angular full-width at half maximum intensity (FWHM) in radians of the (hkl) line profile; θ is the scattering angle (Ling et al. 2019).

TGA

The thermal stability of raw sweet sorghum stalk, crude cellulose (from "Preparation of crude cellulose from sweet sorghum stalk" section), acid-extracted MCC (from "Optimization of MCC extraction by acid hydrolysis" section), refined MCC (from "Purification of acid-extracted MCC by using fibrolytic enzyme treatment" section), and Lowa®PH101 were analyzed by using a thermogravimetric analyzer (STA409C/PC, Netzsch, Germany) under a nitrogen atmosphere at a flow rate of 40 mL/min. The samples (approx. 6 mg) were heated at a heating rate of 10 °C/min from 25 to 900 °C.

^{13}C NMR analysis

^{13}C NMR spectra of refined MCC were recorded using a Bruker Avance III 300WB NMR spectrometer (Germany) operating at 75.42 MHz for 3 h. The measurement conditions were as follows: (1) a rotor spinning speed of 5000 Hz; (2) a contact time of 2 ms; (3) a recycle delay of 2.5 s; and (4) a scan number of 10240. In addition, the spectra were calibrated using tert-butyl carbon atom of adamantane as an external reference (d = 38.48 ppm), and the curve-fitting analysis of ^{13}C spectra were conducted via Peakfit v4.12 software. The relative ^{13}C intensity distribution for solid samples could be determined by the chemical shift regions. Samples were packed in MAS 4 mm diameter zirconia rotors. Chemical shifts are expressed as part per million (ppm) against TMS, which was used as the external standard reference (Zhuang et al. 2019).

Data analysis

Analysis of variance (ANOVA) and Duncan's test were conducted to analyze the differences between various treatments using SPSS (IBM SPSS Statistics 20). Significant difference on factor effect analysis were established at $p = 0.05$ level. The Design-Expert V8.0.6 software was used to process the data and make multiple linear regression.

Results and discussion

Effect of acid extraction parameters on the yield, cellulose content and DP of MCC

The yield, cellulose content and DP of acid-extracted MCC with different settings of extraction parameters (L/S ratio, acid concentration, temperature, and time) were shown in Table 2. The extraction results (yield, cellulose content and DP) during hydrolysis were significantly affected by these four parameters. Overall, the yield and DP of MCC presented a gradual downward trend with the increase of all experiment parameters, which could be because a large amount of protons (H^+) from hydrochloric acid open the fiber structure to facilitate access to cellulose microstructure for depolymerization. H^+ promptly destroyed the outermost amorphous cellulose fiber and hemicellulose, and then further broke down the β-1,4-glycosidic bonds to reach the levelling-off degree of polymerization (LODP). In contrast, the variation trend of cellulose content is upward, which may be due to the removal of impurities, such as hemicellulose and lignin. On the other hand, the higher the acid concentration or high L/S ratio, the more facile is the hydrolysis reaction, which may be attributed to the increased moving amount of H^+ towards β-1,4-glycosidic bond and the weakening effect from Cl^- to the breakdown of glycosidic bonds (Trache et al. 2016; Zhao et al. 2017). In view of thermal effect, the increase of temperature could result in higher efficiency that H^+ broke β-1,4-glycosidic bonds. In other words, higher reaction temperature accelerates the breakdown of cellulose glycosides while the DP and yield decreased correspondingly. Besides, reaction time is an important factor correlated with extraction efficiency and cost. When the time was prolonged from 30 to 90 min, the cellulose content increased sharply from 87.2 to 91.9% because time extension could cause more hydrolysis of both amorphous cellulose and hemicellulose, resulting in the decrease of DP and yield (Klemm et al. 2005). However, if the reaction time continued to increase, the amorphous area would not only be hydrolyzed, but also the crystalline area would be hydrolyzed. Therefore, it is advisable to choose the appropriate reaction time of 90 min which allows for extraction efficiency in the subsequent optimization experiment.

Optimization of acid extraction of MCC with RSM

Statistical analysis and model fitting

Based on the results of single factor test in "Effect of acid extraction parameters on the yield, cellulose content and DP of MCC" section, the reaction time was fixed at 90 min. The remaining three parameters, such as acid concentration, L/S ratio and temperature were further optimized using RSM with the indexes of the yield and cellulose content. As shown in table S1, 17 treatments were conducted with BBD for parameter optimization. As it is well known, MCC is characterized by a high degree of crystallinity of more than 60% and LODP below 350 (Qiang et al. 2016). The LODP of acid-extracted MCC in the single factor test were all below 350 (Table 1), therefore, DP was not evaluated as a response in these optimization experiments.

Table 2 Effect of acid extraction parameters on the yield, cellulose content and DP of MCC

Variable[a]	Level	Yield of MCC (%)	Cellulose content (%)	DP
(1) L/S ratio (mL/g)	10:1	77.43 ± 0.24A	87.56 ± 0.03E	376.36 ± 1.26A
	15:1	76.91 ± 0.56A	88.32 ± 0.10D	329.42 ± 2.58B
	20:1	75.79 ± 0.39B	92.60 ± 0.14C	307.61 ± 1.06C
	25:1	73.91 ± 0.09C	93.38 ± 0.11B	310.13 ± 1.12C
	30:1	73.72 ± 0.34C	95.51 ± 0.44A	288.29 ± 1.06D
(2) Acid concentration (wt%)	1%	79.35 ± 0.20AB	88.11 ± 0.10D	345.99 ± 1.14A
	3%	79.60 ± 0.27A	89.24 ± 0.35C	334.65 ± 0.77B
	5%	79.06 ± 0.33B	91.09 ± 0.07B	315.03 ± 1.00C
	7%	79.07 ± 0.10B	91.64 ± 0.27A	303.02 ± 1.17D
	9%	77.75 ± 0.06C	91.82 ± 0.14A	284.64 ± 0.54E
(3) Temperature (°C)	20	84.12 ± 0.32A	89.84 ± 0.07D	644.72 ± 1.6A
	40	83.95 ± 0.52A	92.95 ± 0.24C	382.79 ± 1.2B
	60	82.64 ± 0.37B	93.50 ± 0.12AB	312.00 ± 1.0C
	80	76.63 ± 0.01C	93.22 ± 0.17BC	297.86 ± 0.3D
	100	70.27 ± 0.62D	93.66 ± 0.28A	291.16 ± 0.7E
(4) Time (min)	30	79.17 ± 0.18A	87.17 ± 0.24C	369.21 ± 1.26A
	50	78.03 ± 0.22B	89.97 ± 0.06B	361.39 ± 0.28B
	70	77.69 ± 0.04B	89.59 ± 0.08B	359.01 ± 0.35C
	90	76.61 ± 0.20C	91.87 ± 0.24A	345.35 ± 0.28D
	110	75.89 ± 0.65D	89.82 ± 0.32B	343.30 ± 1.59E

Different capital letters in the same column indicate significant difference at $p < 0.05$, while he same capital letters indicate insignificant difference at $p > 0.05$

[a]Operation conditions for (1): acid concentration = 7% (wt%), temperature = 60 °C, and time = 90 min, Operation conditions for (2): L/S ratio = 20:1 (mL/g), temperature = 60 °C and time = 90 min, Operation conditions for (3): acid concentration = 7% (wt%), L/S ratio = 20:1 (mL/g) and time = 90 min, Operation conditions for (4): acid concentration = 7% (wt%), L/S ratio = 20:1 (mL/g) and temperature = 60 °C

The fitted equations for the yield (Eq. 5) and cellulose content (Eq. 6) of MCC were given as follows:

$$\begin{aligned} Y_1 = {} & 69.2735 + 2.1307X_1 - 0.7627X_2 \\ & + 4.0072X_3 - 0.0018X_1X_2 + 0.1045X_1X_3 \\ & - 0.0069X_2X_3 - 0.0713X_1^2 + 0.0061X_2^2 \\ & - 0.4088X_3^2 \end{aligned} \quad (5)$$

$$\begin{aligned} Y_2 = {} & 58.8822 + 0.9169X_1 - 0.0037X_2 + 8.2370X_3 \\ & + 0.0034X_1X_2 + 0.0659X_1X_3 - 0.0195X_2X_3 \\ & - 0.0444X_1^2 + 0.0007X_2^2 - 0.5905X_3^2 \end{aligned} \quad (6)$$

Regression analysis and ANOVA were used to fit the models and examine the significance of the parameters and interactions (Luo et al. 2014). R^2, R^2_{adj}, R^2_{pred}, and F values as well as p values were displayed in tables S2 and S3 to evaluate the significance of response surface models. The significant p values of terms lower than 0.01 indicate that the proposed models can properly predict the results of the experiments. The R^2 plus R^2_{adj} can assess the goodness-of-fit for regression models. Based on data presented (tables S2 and S3), it can be concluded that the models were adequate for predicting the yield and cellulose content of MCC in this study (Bondeson et al. 2006; Ko et al. 2015).

Optimization analysis of operation parameters for acid extraction of MCC

As shown in figures S1 and S2, 3D response surface and 2D contour plots were employed to demonstrate

the interactions of the variables and to determine the optimum level of each variable to achieve maximum responses. RSM results showed the optimum operation parameters for acid extraction of MCC were L/S ratio = 17.3:1, temperature = 40 °C, and acid concentration = 7.3%.

Model verification

This above-mentioned optimum condition in "Optimization analysis of operation parameters for acid extraction of MCC" section was slightly modified and used to verify the predictability of the models. Under the modified optimum condition (i.e., L/S ratio = 17.3:1, temperature = 40 °C and acid concentration = 7.0%), the experimental yield and cellulose content of MCC from sweet sorghum stalk were 81.8 and 93.2%, respectively, which were quite consistent with the predicted results (Table 3).

Refining acid-extracted MCC by using fibrolytic enzyme treatment

MCC is as partially depolymerized cellulose, which could still contain a certain amount of impurities, such as amorphous cellulose and hemicellulose. Therefore, the fibrolytic enzyme was used to remove the residual impurities in order to further improve the purity of MCC. The effect of fibrolytic enzyme dosage and treatment time on the purity was shown in Fig. 1a. When the dosage of fibrolytic enzyme was fixed, the residual hemicellulose and other impurities were gradually decomposed and removed, therefore, the purity of extracted MCC increased gradually with the extension of time. The increased enzyme dosage from 2000 to 4000 U/g resulted in the increase of cellulose content. However, further increase of the enzyme dosage to 6000 U/g led to decreased cellulose content in extracted MCC.

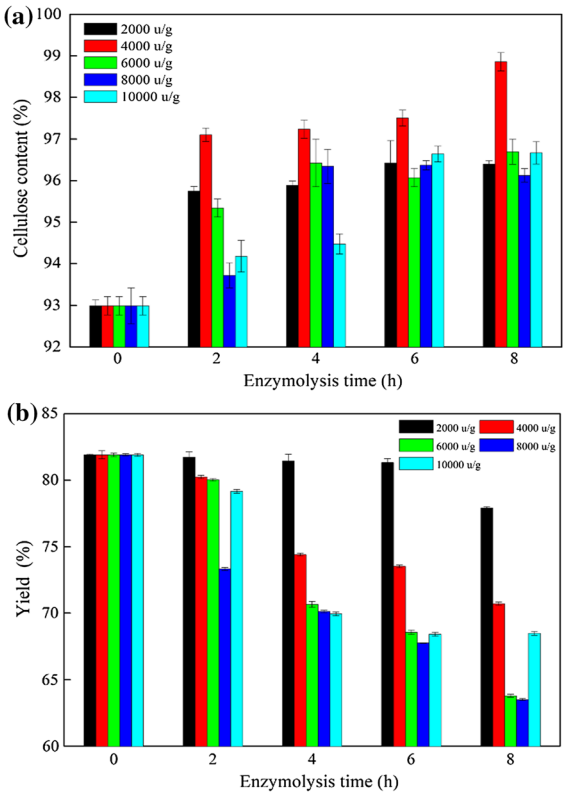

Fig. 1 Effects of enzyme dosage and enzymolysis time on the cellulose content (**a**) and yield (**b**) of refined MCC

As shown in Fig. 1b, the yield decreased with the increase of enzyme dosage and time extension, which was in accordance with the result reported by Agblevor et al. (2007). Therefore, the optimum enzyme treatment condition was enzyme dosage = 4000 U/g and treatment time = 2 h. Under this condition, the yield, cellulose content and DP of the refined MCC obtained by fibrolytic enzyme treatment reached 80.0%, 99.8% and 287, respectively, which is well in agreement with the pharmacopeia specifications of MCC in China and US (> 97%). In comparison with the results reported in literatures (Table 4), the cellulose content of the refined MCC obtained

Table 3 Predicted and experimental values of the responses at optimum conditions

Factors and responses	Optimum conditions	Modified conditions
X_1: Liquid–solid ratio (mL/g)	17.27:1	17.30:1
X_2: Temperature (°C)	40	40
X_3: Hydrochloric acid concentration (%, w/w)	7.27	7.00
Yield of MCC (%)	81.37	81.78 ± 0.28
Cellulose content in MCC (%)	93.01	93.24 ± 0.24

from sweet sorghum stalk by using combined acid-enzyme extraction were higher than that of MCC from wood pulp by single HCl hydrolysis, indicating that the combined acid-enzyme extraction is better than acid extraction only for MCC production.

Characterization of MCC

SEM analysis

The morphological differences of raw stalk, crude cellulose, acid extracted MCC, refined MCC, and Lowa®PH101 were studied with SEM and showed in Fig. 2. It seems that the surface morphology of raw stalk exhibited an irregular aggregation shape in fibrils and rough furrow on the surface area. When the raw stalk sample underwent chemical reagent treatment, the surface morphology changed in terms of size and level of smooth-ness. There are flat ribbon-like and plain uniform structure with slight wrinkles on the surface of crude cellulose and acid extraction MCC, which may be caused by the removal of outer non-cellulosic compounds (hemicellulose, lignin, pectin and wax) surrounding cellulose fiber. Therefore, the internal structure of the cellulose was exposed (Kaushik et al. 2010). On the other hand, the acid extraction MCC also showed well defined plated shaped fibrous network structure. Figure 2d clearly showed the micromorphology of the refined MCC was mostly rod-like or long cylindrical-shaped, and there were a small amount sheet structure as similar with commercial MCC.

FTIR analysis

Different stages of treatment of stalk were examined using FTIR spectroscopy (Fig. 3). For all five samples, the absorption peaks at about 3410 cm^{-1} and 2910 cm^{-1} can be observed. The peak at 3410 cm^{-1} corresponds to the hydrogen-bonded O–H stretch vibrations (Sain and Panthapulakkal 2006; Sun et al. 2005; Xiao et al. 2001) while the peak at 2910 cm^{-1} is due to the aliphatic saturated C–H stretching vibration in lignin and polysaccharides (cellulose and hemicelluloses). The peak at 1730 cm^{-1} for the raw stalk is attributed to either the acetyl and uronic ester groups of the hemicelluloses or the ester linkage of carboxylic group of the ferulic and *p*-coumeric acids of lignin and/or hemicellulose (Alemdar and Sain 2008). This peak is almost absent in the spectra of the chemically (acid) and biological (enzyme) treated celluloses, which indicates nearly complete cleavage of these ester bonds. The characteristics of these acetyl and uronic ester groups almost completely disappeared in

Table 4 Comparison of cellulose content of MCC samples from different starting materials

Sources of MCC	Cellulose content (mass%)	Yield (%)	Reference
Birch sulphite pulp	97.3↓	No data	Nsor-Atindana et al. (2017)
Coniferous sulphite pulp	98.8↓	No data	Nsor-Atindana et al. (2017)
Coniferous kraft pulp	98.6↓	No data	Nsor-Atindana et al. (2017)
Poplar kraft pulp	97.6↓	No data	Nsor-Atindana et al. (2017)
Aspen kraft pulp	97.5↓	No data	Nsor-Atindana et al. (2017)
Cotton linters	99.8 =	No data	Nsor-Atindana et al. (2017)
Flax cellulose	99.6 =	No data	Nsor-Atindana et al. (2017)
Corn husk fibres	98.2↓	No data	Leppänen et al. (2009)
Waste cotton fabrics	No data	85.5↑	Shi et al. (2018)
Waste cotton fabrics	No data	78.1	Xiong et al. (2012)
Waste cotton fabrics	No data	83.4–84.1↑	Hou et al. (2019)
Bleached chemical	88.5–91.9↓	77.5–80.1↓	Yue et al. (2019)
Tea waste	No data	86.7↑	Zhao et al. (2017)
Sweet sorghum stalk	99.8	80.0	This research

"↓" means the cellulose content or yield lower than that of the present study; "=" means equivalence of the cellulose content or yield compared with the present study; "↑" means the cellulose content or yield higher than that of the present study

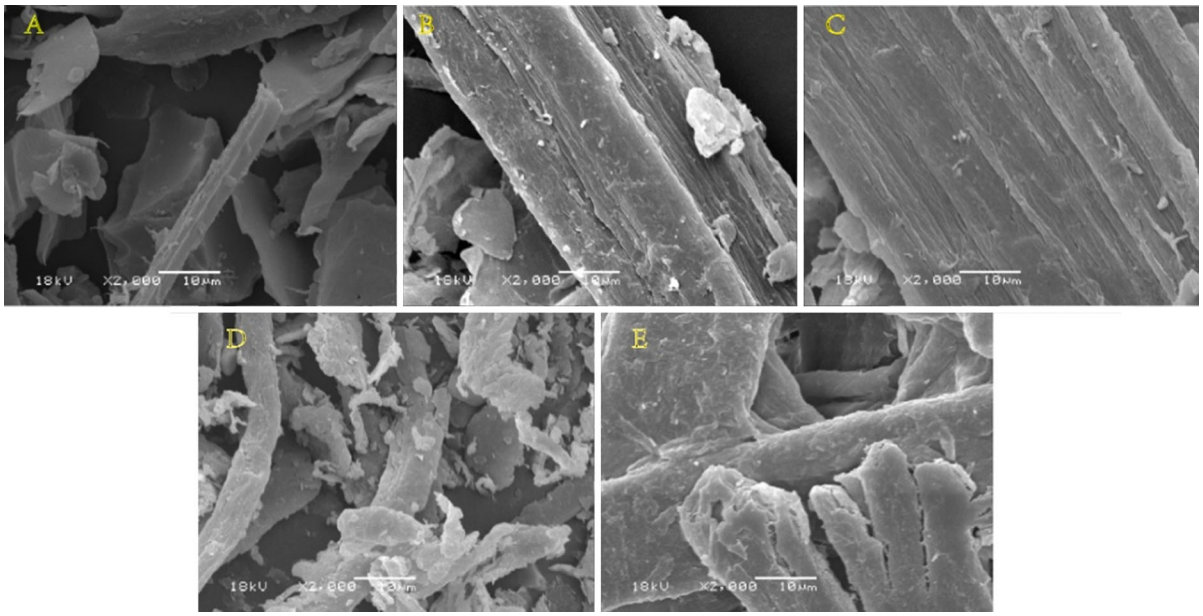

Fig. 2 SEM imaging (×2000): **a** raw stalk, **b** crude cellulose, **c** acid-extracted MCC, **d** refined MCC, and **e** Lowa®PH101

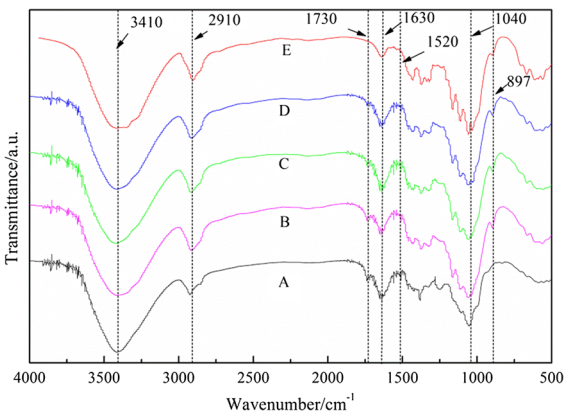

Fig. 3 FTIR spectra of (A) raw stalk, (B) crude cellulose, (C) acid-extracted MCC, (D) refined MCC, and (E) Lowa®PH101

Lowa®PH101, acid-extracted MCC and refined MCC, indicating that most of the impurities were removed. The peak at 1630 cm^{-1} may be due to the bending mode of the absorbed water and carboxylate groups (Sun et al. 2005). In the spectra of refined MCC and Lowa®PH101, no peaks correspond with CH_2 scissors were found at 1520 cm^{-1}, which means that the impurities have been completely removed. The peak at about 1040 cm^{-1} is the characteristic peak of xylan caused by the telescopic vibration of C–OH. Since the main component of hemicellulose is xylan, the change of absorption peak at 1040 cm^{-1} indicates the hydrolysis degree of hemicellulose. The increase of the peak intensity at 897 cm^{-1} in chemically treated stalk fibers, including crude cellulose, acid-extracted or refined MCC, indicates the typical structure of cellulose (due to β-glycosidic linkages of glucose ring within cellulose) (Gañán et al. 2004).

X-ray diffraction

The crystallinity index and crystallite sizes of raw stalk and cellulose obtained at different extraction stage were analyzed by XRD (showed in Table 5 and Fig. 4). According to the report of Klemm et al. (2005), the characteristics structure of cellulose I fiber were typical peaks at 2θ = 14.8° and 22.5°. As shown in Fig. 4, the diffraction patterns of crude cellulose, acid-extracted MCC, refined MCC show peaks at about 16.2° and 22.3°, which represent typical structure of cellulose I. Also, the smooth pattern at around 20°–21° suggested that the preferred orientation for each sample was obvious (French 2014). However, raw stalk did not show a peak value at about 16°. For the raw stalks, large amounts of lignin and other biomass matrix were connected around cellulose microfibrils, causing the mixture of the two distinctive cellulose I peaks (14.8° and 16°). On the other hand,

Table 5 Crystallinity index (*CrI*) of sweet sorghum stalk and cellulose obtained at different extraction stage during MCC preparation

	CrI (%)	Crystallite sizes (nm)
Sweet sorghum stalk	27.65	3.67
Crude cellulose from sweet sorghum stalk	76.40	4.17
Acid extracted MCC	75.19	4.23
Acid-enzyme combination extracted MCC	89.43	4.04
Lowa®PH101	90.69	3.84

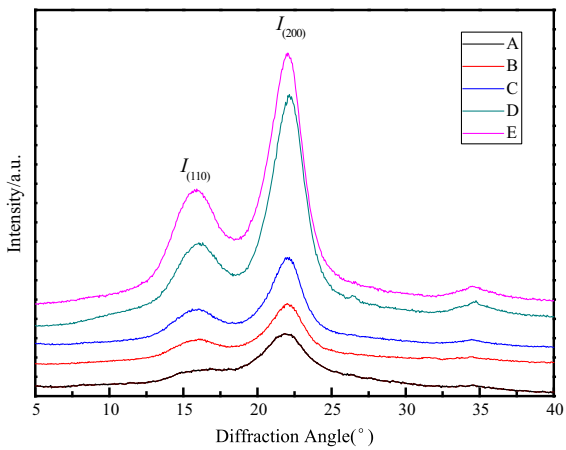

Fig. 4 XRD patterns of (A) raw stalk, (B) crude cellulose, (C) acid-extracted MCC, (D) refined MCC, and (E) Lowa®PH101

the peaks at around 2θ = 22.3° in acid-extracted MCC and refined MCC were more pointed than that of raw stalk and crude cellulose. As shown in Table 5, the value of crystallinity index for raw stalk, crude cellulose, acid-extracted MCC, refined MCC, and Lowa®PH101, which were found to be 27.65%, 76.40%, 75.19%, 89.43% and 90.69%, respectively. These results clearly demonstrate that the crystallinity progressively increases during preparation of refined MCC from sweet sorghum, which is due to the removal of amorphous cellulose and non-cellulose components (e.g. lignin and hemicellulose). In addition, the crystallinity index of refined MCC and commercial Lowa®PH101 are almost the same. The values for the crystallite sizes are also summarized in Table 5. The increase trend of the crystallite sizes during the preparation of acid-extracted MCC particles from sweet sorghum might be associated with a reduction in the corresponding amorphous region. Similarly, the increased crystal size during acid hydrolysis was also reported by Trache et al. (2014). However, the crystallite sizes of refined MCC slightly decreased as compared with acid extracted MCC, which was due to that a small amount of cellulose was degraded by fibrolytic enzyme during purifying process. In addition, the crystalline size of refined MCC from sweet sorghum were higher than those obtained for the commercial Lowa®PH101, which may be the consequence of different materials and preparation technology. In brief, during the extraction process of MCC, the lignin-hemicellulose-cellulose interactions were disrupted, and the consecutive action of alkaline treatment, acid hydrolysis and enzyme purification resulted in the removal of the residual hemicellulose. In the meantime, the lignin was all eliminated, therefore, the high purity MCC was extracted from sweet sorghum stalk.

Thermal analysis

TGA allows us to obtain information about how the thermal stability of the material changes during extraction of MCC from sweet sorghum stalk. The TG and DTG patterns of raw stalk, crude cellulose, acid-extracted MCC, refined MCC, and Lowa®PH101 are shown in Fig. 5. All samples exhibited similar thermal behavior and the progressive extraction of MCC led to the gradual enhancement of the thermal stability. All samples exhibit a small weight loss below 100 °C (Fig. 5a), which can be attributed to the loss of moisture of the samples. For raw stalk, the main decomposition stage was in the range of 170–360 °C and the first degradation step around 180–300 °C can be ascribed to the decomposition of hemicellulose and a part of the lignin fraction, while the main decomposition stage of refined MCC appeared later and were

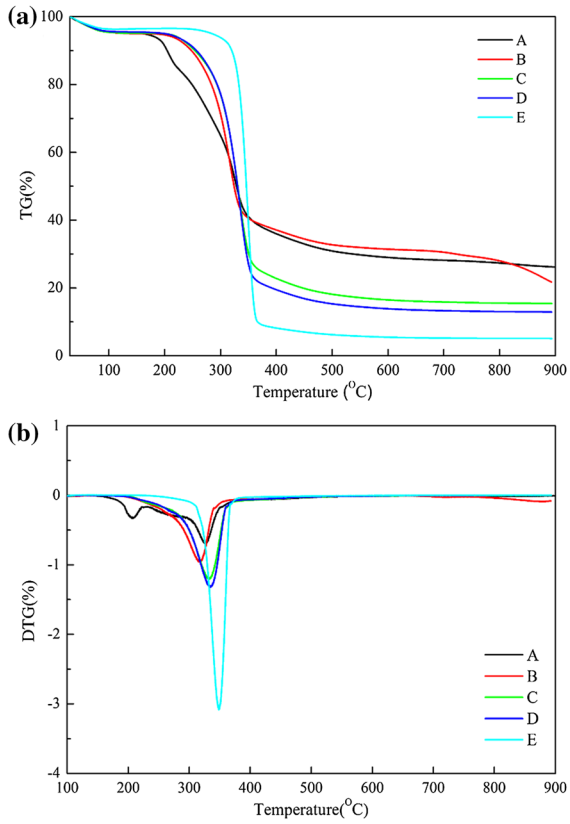

Fig. 5 TGA **a** and DTG **b** curves of (A) raw stalk, (B) crude cellulose, (C) acid-extracted MCC, (D) refined MCC, and (E)Lowa®PH101

observed in the range of 210–350 °C because of the decomposition of cellulose, such as the dehydration, decarboxylation, depolymerization, and decomposition of glycosyl units followed by the formation of a charred residue. In addition, there is a significant difference in the residual mass between refined MCC (13.65%) and raw stalk (27.38%), crude cellulose (31.26%), acid-extracted MCC (14.89%) after 500 °C. The relatively small residue in refined MCC compared to raw stalk may be due to partial removal of waxy or ash. However, the residual mass of refined MCC (more than 18%) at temperature around 500–800 °C were remarkably higher than that (about 5%) of Lowa®-PH101. This finding can be explained by the compositional difference, given that thermal degradation of cellulose-based fiber is significantly influenced by its structure and composition (Collazo-Bigliardi et al. 2018).

As showed in Fig. 5b (DTG curves), the peak around 335–350 °C is attributed to cellulose and lignin decomposition in all samples. Two decomposition peaks at 200 °C and 335 °C in raw stalk were observed associated to the successive degradation of the different lignocellulosic fractions. Mansaray and Ghaly (1998) reported that lignocellulosic materials decompose in the temperature range of 150–500 °C. Specifically, hemicellulose and cellulose decompose mainly in the range of 150–350 °C and 275–350 °C, respectively while lignin undergoes gradual decomposition in the range of 250–500 °C. However, only one peak appeared in crude cellulose, acid-extracted MCC and refined MCC according to DTG in Fig. 5b, which can be attributed to the loosening of the low molecular weight lignin fragments (Johar et al. 2012), suggesting that there is only one type of crystal in crude cellulose, acid-extracted MCC, refined MCC, and Lowa®PH101. It is noteworthy that the acid extraction followed enzymatic hydrolysis resulted in a significant increase in degradation temperature, which could be due to the removal of hemicellulose and lignin fractions and the increase of cellulose content. The degradation peaks of Lowa®PH101 are narrower than those of refined MCC, indicating the presence of more homogeneous crystals in Lowa®PH101. According to the TGA and DTG results, the refined MCC has good thermal stability and will be a potential bio-based material to produce "green" bio-composites.

^{13}C NMR spectra

NMR spectroscopy is used to measure the absorption of radiofrequency radiation by atomic nuclei together with a nonzero spins in a strong magnetic field. In general, the peaks in the region between 60 and 105 ppm are due to the different carbons of cellulose, and the peaks of carbon cellulose C1, C4, and C6 are around δ102–108 ppm, δ80–92 ppm, and δ57–67 ppm, respectively (Trache et al. 2016). The ^{13}C NMR spectra of the refined MCC from sweet sorghum was showed in figure S3. The ^{13}C NMR spectrum is almost identical to that of hydrothermal treated MCC (P = 1.8 MPa, T = 210 °C) reported by Seehra et al. (2014), indicating that the chemical phase of the refined MCC is still cellulose. The refined MCC from sweet sorghum is assigned to the C1 (106.07 ppm), C4 (84.74 ppm) and C6 (64.33 ppm) carbons from the downfield side except for a cluster of

resonances in the range 73–76 ppm, corresponding to the C2, C3 and C5 carbons. Moreover, the downfield and upfield contributions are referred to as C4 and C6, respectively (Yamamoto et al. 2006).

Conclusions

Sweet sorghum are rich in cellulose and annually available crop stalk and thus can be a potential raw material for MCC production. The present study revealed that the high quality refined MCC prepared by combined acid-enzyme hydrolysis with very minimum chemical usage. Under the optimal hydrochloric acid condition (acid concentration = 7.0%, L/S ratio = 17.3:1, time = 90 min, and temperature = 40 °C), the yield, cellulose content and the DP of acid extracted MCC could be 81.78%, 93.24% and 315, respectively. Further refining of acid extracted MCC by fibrolytic enzyme led to the cellulose content of extracted MCC increased to 99.80%, the yield and DP of the extracted MCC were slightly decreased to 80.03% and 287, respectively, which was consistent with the national and international pharmacopeia standards. The structural characterization studies showed that the rod-shaped like MCC from sweet sorghum showed typical of cellulose I structure and had a series of characteristic chemical groups as similar with commercial Lowa®PH101. The MCC sample prepared exhibits good thermal stability properties, thus making it promising candidate for use in many fields. The present study provides a promising method to extract MCC from sweet sorghum, which would be an alternative way for sustainable use of sweet sorghum.

Acknowledgments This work was financially supported by the National Natural Science Foundation of China (51666010, 51366009), China Postdoctoral Science Foundation Funded Project (2018M631217), Natural Science Foundation of Gansu Province (17JR5RA117, 18JR3RA150), and Hong Liu Excellent Young Cultivation Project of Lanzhou University of Technology (YQ2018). Thanks for kindly help from Dr. Zhe Ling (Nanjing Forestry University) on XRD analysis.

References

Agblevor FA, Ibrahim MM, El-Zawawy WK (2007) Coupled acid and enzyme mediated production of microcrystalline cellulose from corn cob and cotton gin waste. Cellulose 14:247–256. https://doi.org/10.1007/s10570-006-9103-y

Alemdar A, Sain M (2008) Isolation and characterization of nanofibers from agricultural residues: wheat straw and soy hulls. Bioresour Technol 99(6):1664–1671. https://doi.org/10.1016/j.biortech.2007.04.029

Anglani C (1998) Sorghum for human food—a review. Plant Food Hum Nutr 52(1):85–95. https://doi.org/10.1023/a:1008065519820

Ariyajaroenwong P, Laopaiboon P, Jaisil P, Laopaiboon L (2012) Repeated-batch ethanol production from sweet sorghum juice by *Saccharomyces cerevisiae* immobilized on sweet sorghum stalks. Energies 5(4):559–566. https://doi.org/10.3390/en5041215

Azubuike CP, Okhamafe AO (2012) Physicochemical, spectroscopic and thermal properties of microcrystalline cellulose derived from corn cobs. Int J Recycl Org Waste Agric 1(1):106–115. https://doi.org/10.1186/2251-7715-1-9

Bondeson D, Mathew A, Oksman K (2006) Optimization of the isolation of nanocrystals from microcrystalline cellulose by acid hydrolysis. Cellulose 13(2):171. https://doi.org/10.1007/s10570-006-9061-4

Chuayjuljit S, Su-Uthai S, Charuchinda S (2010) Poly (vinyl chloride) film filled with microcrystalline cellulose prepared from cotton fabric waste: properties and biodegradability study. Waste Manag Res 28(2):109–117. https://doi.org/10.1177/0734242x09339324

Collazo-Bigliardi S, Ortega-Toro R, Boix AC (2018) Isolation and characterisation of microcrystalline cellulose and cellulose nanocrystals from coffee husk and comparative study with rice husk. Carbohydr Polym 191:205–215. https://doi.org/10.1016/j.carbpol.2018.03.022

Das K, Ray D, Bandyopadhyay NR, Ghosh T, Mohanty AK, Misra M (2009) A study of the mechanical, thermal and morphological properties of microcrystalline cellulose particles prepared from cotton slivers using different acid concentrations. Cellulose 16(5):783–793. https://doi.org/10.1007/s10570-009-9280-6

Elsakhawy M, Hassan ML (2007) Physical and mechanical properties of microcrystalline cellulose prepared from agricultural residues. Carbohydr Polym 67(1):1–10. https://doi.org/10.1016/j.carbpol.2006.04.009

Fazaeli H, Golmohhammadi HA, Almoddarres A, Mosharraf S, Shoaei AA (2006) Comparing the performance of sorghum silage with maize silage in feedlot calves. Pak J Biol Sci 9(13):2450–2455. https://doi.org/10.3923/pjbs.2006.2450.2455

French AD (2014) Idealized powder diffraction patterns for cellulose polymorphs. Cellulose 21:885–896. https://doi.org/10.1007/s10570-013-0030-4

Gañán P, Cruz J, Garbizu S, Arbelaiz A, Mondragon I (2004) Stem and bunch banana fibers from cultivation wastes: effect of treatments on physico-chemical behavior. J Appl Polym Sci 94(4):1489–1495. https://doi.org/10.1002/app.21061

Gu P, Xu S, Zhou S, Liu Z, Sun Y, Ou N, Hu Y, Liu J, Wu Y, Wang X, Wang D (2017) Optimization of angelica sinensis polysaccharide-loaded poly (lactic-co-glycolicacid) nanoparticles by RSM and its immunological activity

in vitro. Int J Biol Macromol 107:222–229. https://doi.org/10.1016/j.ijbiomac.2017.08.176

Hamid SBA, Chowdhury ZZ, Karim MZ, Karim MZ (2014) Catalytic extraction of microcrystalline cellulose (MCC) from *Elaeis guineensis* using central composite design (CCD). Bioresources 9(4):7403–7426. https://doi.org/10.15376/biores.9.4.7403-7426

Hou WS, Ling C, Shi S, Yan ZF (2019) Preparation and characterization ofmicrocrystalline cellulose fromwaste cotton fabrics by using phosphotungstic acid. Int J Biol Macromol 123:363–368. https://doi.org/10.1016/j.ijbiomac.2018.11.112

Ibrahim MM, El-Zawawy WK, Jüttke Yvonne, Koschella A, Heinze T (2013) Cellulose and microcrystalline cellulose from rice straw and banana plant waste: preparation and characterization. Cellulose 20(5):2403–2416. https://doi.org/10.1007/s10570-013-9992-5

Ilindra A, Dhake JD (2008) Notes microcrystalline cellulose from bagasse and rice straw. Indian J Chem Technol 15(5):497–499. https://doi.org/10.2298/hemind08053131

Ilyas RA, Sapuan SM, Ishak MR (2018) Isolation and characterization of nanocrystalline cellulose from sugar palm fibres (*Arenga pinnata*). Carbohydr Polym 181:1038–1051. https://doi.org/10.1016/j.carbpol.2017.11.045

Jiang D, Hao MM, Fu JY, Liu K, Yan XX (2019) Potential bioethanol production from sweet sorghum on marginal land in China. J Clean Prod 220:225–234. https://doi.org/10.1016/j.jclepro.2019.01.294

Johar N, Ahmad I, Dufresne A (2012) Extraction, preparation and characterization of cellulose fibres and nanocrystals from rice husk. Ind Crop Prod 37(1):93–99. https://doi.org/10.1016/j.indcrop.2011.12.016

Kalita RD, Kalita RD, Nath Y, Ochubiojo ME, Buragohain AK (2013) Extraction and characterization of microcrystalline cellulose from fodder grass; *Setaria glauca* (L) P. Beauv, and its potential as a drug delivery vehicle for isoniazid, a first line antituberculosis drug. Colloids Surf B Biointerfaces 108(4):85–89. https://doi.org/10.1016/j.colsurfb.2013.02.016

Kambli ND, Mageshwaran V, Patil PG, Saxena S, Deshmukh RR (2017) Synthesis and characterization of microcrystalline cellulose powder from corn husk fibres using biochemical route. Cellulose 24(12):5355–5369. https://doi.org/10.1007/s10570-017-1522-4

Kaushik A, Singh M, Verma G (2010) Green nanocomposites based on thermoplastic starch and steam exploded cellulose nanofibrils from wheat straw. Carbohydr Polym 82(2):337–345. https://doi.org/10.1016/j.carbpol.2010.04.063

Kian LK, Jawaid M, Ariffin H, Alothman OY (2017) Isolation and characterization of microcrystalline cellulose from roselle fibers. Int J Biol Macromol 103:931–940. https://doi.org/10.1016/j.ijbiomac.2017.05.135

Kiziltas A, Gardner DJ, Han Y, Yang HS (2014) Mechanical properties of microcrystalline cellulose (MCC) filled engineering thermoplastic composites. J Polym Environ 22(3):365–372. https://doi.org/10.1007/s10924-014-0676-5

Klemm D, Heublein B, Fink HP, Bohn A (2005) Cellulose: fascinating biopolymer and sustainable raw material. Angew Chem Int Ed 44(22):3358–3393. https://doi.org/10.1002/chin.200536238

Ko WC, Chang CK, Wang HJ, Wang SJ, Hsieh CW (2015) Process optimization of microencapsulation of curcumin in γ-polyglutamic acid using response surface methodology. Food Chem 172(172):497–503. https://doi.org/10.1016/j.foodchem.2014.09.100

Leppänen K, Andersson S, Torkkeli M, Knaapila M, Kotelnikova N, Serimaa R (2009) Structure of cellulose and microcrystalline cellulose from variouswood species, cotton and flax studied by X-ray scattering. Cellulose 16(6):999–1015. https://doi.org/10.1007/s10570-009-9298-9

Li M, Feng SQ, Wu LM et al (2014) Sugar-rich sweet sorghum is distinctively affected by wall polymer features for biomass digestibility and ethanol fermentation in bagasse. Bioresour Technol 167:14–23. https://doi.org/10.1016/j.biortech.2014.04.086

Ling Z, Tuo Wang, Makarem M, Cintron MS, Cheng HN, Kang X, Bacher M, Potthast A, Rosenau T, King H, Delhom CD, Nam S, Edwards JV, Kim SH, Xu F, French AD (2019) Effects of ball milling on the structure of cotton cellulose. Cellulose 26:305–328. https://doi.org/10.1007/s10570-018-02230-x

Luo X, Guan R, Chen X, Tao M, Ma J, Zhao J (2014) Optimization on condition of epigallocatechin-3-gallate (EGCG) nanoliposomes by response surface methodology and cellular uptake studies in Caco-2 cells. Nanoscale Res Lett 9(1):1–9. https://doi.org/10.1186/1556-276x-9-291

Mansaray KG, Ghaly AE (1998) Thermal degradation of rice husks in nitrogen atmosphere. Bio Resour Technol 65(1–2):13–20. https://doi.org/10.1016/s0960-8524(98)00031-5

Merci A, Urbano A, Grossmann MVE, Tischer CA, Mali S (2015) Properties of microcrystalline cellulose extracted from soybean hulls by reactive extrusion. Food Res Int 73:38–43. https://doi.org/10.1016/j.foodres.2015.03.020

Murray SC, Rooney WL, Hamblin MT, Mitchell SE, Kresovich S (2009) Sweet sorghum genetic diversity and association mapping for brix and height. Plant Genome 2(1):48–62. https://doi.org/10.3835/plantgenome2008

Nsor-Atindana J, Chen M, Goff HD, Zhong F, Sharif HR, Li Y (2017) Functionality and nutritional aspects of microcrystalline cellulose in food. Carbohydr Polym 172(9):159–174. https://doi.org/10.1016/j.carbpol.2017.04.021

Qiang D, Zhang M, Li J, Xiu H, Liu Q (2016) Selective hydrolysis of cellulose for the preparation of microcrystalline cellulose by phosphotungstic acid. Cellulose 23(2):1199–1207. https://doi.org/10.1007/s10570-016-0858-5

Regassa TH, Wortmann CS (2014) Sweet sorghum as a bioenergy crop: literature review. Biomass Bioenergy 64:348–355. https://doi.org/10.1016/j.biombioe.2014.03.052

Ren HW, Zhao T, Xing JM, Zhang Y, Li ZZ, Wang YG, Ma WP (2015) Isolation and characterization of microcrystalline cellulose from distillers grains. J Biobased Mater Bioenergy 9(5):515–522. https://doi.org/10.1166/jbmb.2015.1550

Sain M, Panthapulakkal S (2006) Bioprocess preparation of wheat straw fibers and their characterization. Ind Crops

Prod 23(1):1–8. https://doi.org/10.1016/j.indcrop.2005.01.006

Seehra MS, Popp BV, Goulay F, Pyapalli SK, Gullion T, Poston J (2014) Hydrothermal treatment of microcrystalline cellulose under mild conditions: characterization of solid and liquid-phase products. Cellulose 21(6):4483–4495. https://doi.org/10.1007/s10570-014-0424-y

Sheng S, Zhang M, Chen L, Hou W, Yan Z (2018) Extraction and characterization of microcrystalline cellulose from waste cotton fabrics via hydrothermal method. Waste Manage 82:139–146. https://doi.org/10.1016/j.wasman.2018.10.023

Shi S, Zhang M, Chen L, Hou W, Yan Z (2018) Extraction and characterization of microcrystalline cellulose from waste cotton fabrics via hydrothermal method. Waste Manag 82:139–146. https://doi.org/10.1016/j.wasman.2018.10.023

Sun G, French CR, Martin GR, Younghusband B, Green RC, Xie Y, Mathews M, Barron JR, Fitzpatrick DG, Gulliver W, Zhang H (2005) Comparison of multifrequency bioelectrical impedance analysis with dual-energy X-ray absorptiometry for assessment of percentage body fat in a large, healthy population1-3. Am J Clin Nutr 81(1):74–78. https://doi.org/10.1079/phn2004668

Trache D, Donnot A, Khimeche K, Benelmir R, Brosse N (2014) Physico-chemical properties and thermal stability of microcrystalline cellulose isolated from Alfa fibres. Carbohydr Polym 104(1):223–230. https://doi.org/10.1016/j.carbpol.2014.01.058

Trache D, Hussin MH, Hui Chuin CT, Sabar S, Fazita MRN, Taiwo OFA, Hassan TM, Haafiz MKM (2016) Microcrystalline cellulose: isolation, characterization and biocomposites application—a review. Int J Biol Macromol 93(Pt A):789–804. https://doi.org/10.1016/j.ijbiomac.2016.09.056

Updegraff DM (1969) Semimicro determination of cellulose in biological material. Anal Biochem 32(3):420–424. https://doi.org/10.1016/s0003-2697(69)80009-6

Vanhatalo K, Lundin T, Koskimäki A, Lillandt M, Dahl O (2016) Microcrystalline cellulose property–structure effects in high-pressure fluidization: microfibril characteristics. J Mater Sci 51(12):6019–6034. https://doi.org/10.1007/s10853-016-9907-6

Wang D, Shang SB, Song ZQ, Lee MK (2010) Evaluation of microcrystalline cellulose prepared from kenaf fibers. J Ind Eng Chem 16(1):152–156. https://doi.org/10.1016/j.jiec.2010.01.003

Wang J, Zhao Y, Li W, Wang Z, Shen L (2015) Optimization of polysaccharides extraction from *Tricholoma mongolicum* Imai and their antioxidant and antiproliferative activities. Carbohydr Polym 131:322–330. https://doi.org/10.1016/j.carbpol.2015.06.009

Wu LM, Li M, Huang JF et al (2015) A near infrared spectroscopic assay for stalk soluble sugars, bagasse enzymatic saccharification and wall polymers in sweet sorghum. Bioresour Technol 177:118–124. https://doi.org/10.1016/j.biortech.2014.11.073

Xiao B, Xiao B, Sun XF, Sun RC (2001) Chemical, structural, and thermal characterizations of alkali-soluble lignins and hemicelluloses, and cellulose from maize stems, rye straw, and rice straw. Polym Degrad Stab 74(2):307–319. https://doi.org/10.1016/S0141-3910(01)00163-X

Xiong R, Zhang X, Tian D, Zhou ZH, Lu CH (2012) Comparing microcrystalline with spherical nanocrystalline cellulose from waste cotton fabrics. Cellulose 19:1189–1198. https://doi.org/10.1007/s10570-012-9730-4

Yamamoto H, Horii F, Hirai A (2006) Structural studies of bacterial cellulose through the solid-phase nitration and acetylation by cp/mas ^{13}C NMR spectroscopy. Cellulose 13(3):327–342. https://doi.org/10.1007/s10570-005-9034-z

Yue XP, He JC, Xu Y, Yang MX, Xu YJ (2019) A novel method for preparing microcrystalline cellulose from bleached chemical pulp using transition metal ions enhanced high temperature liquid water process. Carbohydr Polym 208:115–123. https://doi.org/10.1016/j.carbpol.2018.12.072

Zhao T, Chen Z, Lin X, Ren Z, Li B, Zhang Y (2017) Preparation and characterization of microcrystalline cellulose (MCC) from tea waste. Carbohydr Polym 184:164–170. https://doi.org/10.1016/j.carbpol.2017.12.024

Zhuang XZ, Zhan H, Song YP, He C, Huang YP, Yin XL, Wu CZ (2019) Insights into the evolution of chemical structures in lignocellulose and non-lignocellulose biowastes during hydrothermal carbonization (HTC). Fuel 236:960–974. https://doi.org/10.1016/j.fuel.2018.09.019